

Nuclear Translocation of Vitellogenin in the Honey Bee (*Apis mellifera*)

Heli Salmela¹, Gyan Harwood^{2,*}, Daniel Münch³, Christine Elsik⁴, Elías Herrero-Galán⁵, Maria K. Vartiainen⁶, Gro Amdam^{3, 7}

¹ Organismal and Evolutionary Biology Research Program, University of Helsinki, Viikinkaari 1, FI-00014, Finland

² Department of Entomology, University of Illinois at Urbana-Champaign, 320 Morrill Hall
505 South Goodwin Avenue, Urbana, IL, 61801, USA

³ Faculty of Environmental Sciences and Natural Resource Management, Norwegian University of Life Sciences, N-1432 Aas, Norway

⁴ College of Agriculture, Food, and Natural Resources, University of Missouri, 2-64 Agriculture Building, Columbia, MO, 65211, USA

⁵ Centro Nacional de Biotecnología, Calle Darwin 3, 28049 Madrid, Spain

⁶ Institute of Biotechnology, Helsinki Institute of Life Science, University of Helsinki, Viikinkaari 5, 00014 Helsinki, Finland

⁷ School of Life Sciences, Arizona State University, 427 E Tyler Mall, Tempe, AZ, 85281, USA

*Corresponding author: Gyan Harwood, Department of Entomology, University of Illinois at Urbana-Champaign, 320 Morrill Hall, 505 South Goodwin Avenue, Urbana, IL 61801

E-mail: gharwood@illinois.edu

1 **Abstract**

2 Vitellogenin (Vg) is a conserved protein used by nearly all oviparous animals to produce eggs. It is also
3 pleiotropic and performs functions in oxidative stress resistance, immunity, and, in honey bees,
4 behavioral development of the worker caste. It has remained enigmatic how Vg affects multiple traits.
5 Here, we asked whether Vg enters the nucleus and acts via DNA-binding. We used immunohistology,
6 cell fractionation and cell culturation to show that a structural subunit of honey bee Vg translocates into
7 cell nuclei. We then demonstrated Vg-DNA binding theoretically and empirically with prediction
8 software and chromatin immunoprecipitation with sequencing (ChIP-seq), finding binding sites at
9 genes influencing immunity and behavior. Finally, we investigated the immunological and enzymatic
10 conditions affecting Vg cleavage and nuclear translocation, and constructed a 3D structural model. Our
11 data are the first to show Vg in the nucleus and suggests a new fundamental regulatory role for this
12 ubiquitous protein.

13

14
15 Key words:
16 Vitellogenin
17 Nuclear protein
18 DNA binding
19

20 **1. Introduction**

21 Vitellogenin (Vg) is an egg yolk precursor protein common to nearly all oviparous animals and
22 likely evolved around 700 million years ago as the oldest member of the Large Lipid Transfer Protein
23 (LLTP) family (Hayward et al., 2010). It is highly pleiotropic, functioning as a storage protein
24 (Amdam and Omholt, 2002), an immunomodulator (Du et al., 2017; Garcia et al., 2010; Li et al.,
25 2008), an antioxidant (Havukainen et al., 2013; Salmela et al., 2016), and a behavior regulator (Amdam
26 et al., 2006; Antonio et al., 2008; Nelson et al., 2007). These functions are observed in taxa as disparate
27 as fish, corals, and insects, suggesting that Vg may have evolved to support multiple functions. Honey
28 bees (*Apis mellifera*) have been the premier insect model for studying Vg pleiotropy, owing largely to
29 the central role it plays in colony division of labor. Here, the non-reproductive worker caste performs a
30 series of age-dependent tasks that is regulated, in part, by Vg titers circulating in their hemolymph
31 (Nelson et al., 2007).

32 The cause of Vg's pleiotropy remains somewhat enigmatic. We have detailed understanding on
33 how Vg forms egg yolk (Tufail and Takeda, 2008), and how it acts in innate immunity as a pathogen
34 pattern recognition receptor (Li et al., 2008), but the molecular mechanism(s) by which it influences
35 multiple traits remains unclear. Some pleiotropic proteins implement their multiple effects by acting as
36 transcription factors via DNA-binding or participating in gene-regulatory complexes that affect the
37 expression of many genes (Chesmore et al., 2016). Interestingly, down-regulation of honey bee Vg by
38 means of RNA-interference mediated *vg* gene knockdown alters the expression of thousands of genes
39 (Wheeler et al., 2013). However, no previous research has addressed or established whether Vg can
40 translocate into the cell nucleus and bind DNA. This lack of investigation may be due to Vg's large
41 size, as the proteins are typically around 200 kDa (Tufail and Takeda, 2008), while most passively-
42 transported nuclear proteins are below 60 kDa (Wang and Brattain, 2007). Yet in many animals, Vg is

43 enzymatically cleaved and reassembled prior to secretion (Tufail and Takeda, 2008). In invertebrates
44 such as insects, Vg is cleaved in the vicinity of a multiply phosphorylated polyserine linker sequence
45 stretch that resides between two evolutionarily conserved Vg protein domains called the N-sheet and
46 the α -helical domain (Baker, 1988; Havukainen et al., 2012; Tufail and Takeda, 2008). In honey bees,
47 this cleavage occurs *in vivo* in the fat body, the primary production site of Vg (Tufail and Takeda,
48 2008), and results in a detached 40 kDa N-sheet (Havukainen et al., 2011). The function of this N-sheet
49 is not fully known, but in fish it serves as the receptor binding region (Li et al., 2003).

50 In this study, we asked whether pleiotropic effects of Vg may be partly explained by nuclear
51 translocation and DNA-binding of the conserved N-sheet, and we used the honey bee as our study
52 organism. First, we used confocal microscopy and Western blots of nuclear compartments to test
53 whether the N-sheet subunit can translocate into the nucleus of fat body cells, using an antibody
54 targeting the honey bee N-sheet. We verified these results by observing nuclear uptake of fluorescently
55 labelled Vg in cell culture. Second, we predicted the DNA-binding capability of honey bee Vg using
56 sequence- and structure-based software, and then used ChIP-seq to identify Vg binding sites in honey
57 bee DNA. We compared workers <24 h old and 7 days old to determine whether Vg-DNA binding
58 sites persist as workers transition between behavioral tasks. We searched for *de novo* binding motifs
59 and performed a gene ontology analysis of Vg-DNA binding sites, identifying many sites associated
60 with immune- and behavior- related genes. These data motivated a functional response-to-challenge
61 assay using *E. coli* to reveal if behavior of Vg cleavage and translocation is, in fact, dynamic. Finally,
62 we established the enzymatic conditions required for Vg cleavage, and we developed a three-
63 dimensional structure model to elucidate the critical N-terminal area of the protein.

64 **2. Material and Methods**

65 *2.1 Antibody against honey bee Vg 40 kDa N-sheet*

66 The honey bee Vg 40 kDa fragment (Uniprot ID Q868N5; the amino acid residues 24-360) was
67 produced in *E. coli* by GenScript (Piscataway, NJ, USA); it was subcloned into pUC57 vector, and an
68 N-terminal hexahistidine tag was used for one-step affinity purification. The polyclonal serum antibody
69 was raised in a rat by Harlan Laboratories (Boxmeer, the Netherlands), and tested by Western blotting
70 against proteins extracted from the honey bee (see S1).

71

72 *2.2 Immunohistology*

73 N=6 winter worker bees were collected from two hives at Norwegian University of Life Sciences, Aas,
74 Norway. The gut was removed, and the abdomen detached and placed for overnight fixing in 4%
75 paraformaldehyde in 4 °C, followed by three PBS washes, 10 min each. The fat body was dissected in
76 PBS and de/rehydrated with a full ethanol series. For each individual, one tissue sample was used as
77 test (primary and secondary antibodies) and another one as control (no primary antibody). The samples
78 were incubated with the primary antibody overnight in 4°C (1:50 in 2 % BSA-PBS-Triton X-100).
79 DAPI was used as a nuclear marker. The anti-rat secondary antibody was Alexa-568 nm that has no
80 emission spectrum overlap with DAPI. For qualitative anatomical descriptions, a high NA (=high
81 resolution) objective was chosen (40x immersion oil; NA 1.25). Scans were taken with zoom 1.0 and
82 zoom 2.0. All images were taken in sequential acquisition mode to minimize crosstalk between the two
83 channels for detecting DAPI and the Vg signal.

84

85 *2.3 Cell fractionation*

86 Nine winter worker honey bee individuals were anesthetized in cold and the fat body tissue was
87 dissected in ice cold PBS. Tissues were placed in three tubes with 50 µl hypotonic buffer (20 mM Tris-
88 HCl pH 7, 10 mM NaCl and 3 mM MgCl₂) pooling three individuals per tube. 2.5 µl 10 % NP-40 was
89 added, followed by 10 s vortex and centrifugation for 10 min 3000 g in 4°C. The supernatant was

90 collected as the cytosolic fraction. The pellet was washed once with 500 μ l hypotonic buffer, and then
91 suspended in 30 μ l hypotonic buffer with 5 mM EDTA, 1 % Tween-20 and 0.5 % SDS and vortexed.
92 All samples were then centrifuged for 10 min 15000 g in 4°C. 15 μ l of each sample was run on SDS-
93 PAGE gel and blotted.

94

95 *2.4 Western blotting*

96 The gel and Western blot reagents were purchased from Bio-Rad, and the protocol for all blots was as
97 follows: The blotted nitrocellulose membrane was incubated with PBS containing 0.5% Tween with
98 2.5% bovine serum albumin overnight. The membrane was incubated for 1 h with the N-sheet antibody
99 (1:2000) and for 1 h with a horseradish peroxidase-conjugated secondary antibody (1:5000) prior to
100 imaging using an Immun-Star kit. All gels and blots were imaged, and band intensities were measured
101 using a ChemiDoc XRS imager (Bio-Rad).

102

103 *2.5 Whole Vg purification*

104 Vg was purified from wintertime worker honey bee hemolymph as in Salmela *et al.* 2015.

105

106 *2.6 Labeled Vg in cell culture*

107 Pure Vg was labeled with Alexa Fluor 488 protein labeling kit (Invitrogen, Carlsbad, CA, USA).
108 HighFive cells were grown on an 8-well chamber slide (Thermo Fisher) overnight (number of slides
109 one, repeated three times). The media was replaced with 20 μ g/ μ l Vg-488 in PBS and incubated in dark
110 for 1 h. The cells were washed twice with PBS, fixed with 4 % paraformaldehyde and the washes were
111 repeated. DAPI was used as a nuclear marker. The cells were imaged the following day with Leica
112 TCS SP5 MP (63x).

113

114 2.7 *DNA-binding prediction*

115 The following prediction tools available for protein-DNA binding were tested with default settings:
116 Sequence-based DNABIND (Liu and Hu, 2013), DP-BIND (Hwang et al., 2007) and DRNApred (Yan
117 and Kurgan, 2017), and structure-based DNABIND (Liu and Hu, 2013) and DISPLAR (Tjong and
118 Zhou, 2007). The structure used was the honey bee Vg N-sheet homology model published earlier
119 (Havukainen et al., 2011).

120

121 2.8 *ChIP-seq*

122 To test empirically whether Vg binds to DNA, and to determine what types of genes and genomic
123 regions Vg is bound to, we performed ChIP-seq on newly emerged (<24 hours) and 7-day old worker
124 bees. Newly emerged workers will take on tasks such as cleaning comb cells, while workers at 7 days
125 old act as nurses to nourish the queen and developing larvae. Thus, workers in these two age groups
126 span an important behavioral transition or maturation that is integral to a colony's division of labor.
127 Samples were created by pooling fat body tissue from 10 individuals from each age group, all
128 originating from the same hive. Freshly harvested samples were flash frozen in liquid nitrogen and
129 homogenized. ChIP was carried out with established protocols (Bai et al., 2013) using Dynabeads™
130 Protein G (Invitrogen). We opted to use polyclonal antibodies raised in rabbits against the whole 180
131 kDa Vg molecule (Pacific Immunology, Ramona, CA) (Jensen and Børgesen, 2000) rather than the rat-
132 origin antibodies against the 40 kDa Vg N-terminal domain used elsewhere in this study because of
133 their superior immunoprecipitation performance. In a preliminary study, the rabbit-origin whole-Vg
134 antibodies consistently pulled down more chromatin than multiple batches of the rat-origin Vg N-
135 terminal antibodies, which failed to retrieve sufficient chromatin for sequencing. This is likely due to
136 Protein G (and A) having a greater affinity for rabbit-origin than rat-origin antibodies, as per the
137 manufacturer. As a negative control, we compared immunoprecipitated DNA against input DNA (i.e.,

138 DNA from the same sample not precipitated with antibodies). We opted against using anti-GFP
139 antibodies in our negative control, as this type of negative control is less commonly used and more
140 prone to background noise (Xu et al., 2021).

141 Chromatin samples were sequenced at the DNASU lab at Arizona State University. The raw
142 Illumina 2x75bp pair-end reads were quality checked using FastQC v0.10.1 (Andrews, 2010), followed
143 by adapter trimming and quality clipping by Trimmomatic 0.35 (Bolger et al., 2014). Any reads with
144 start, end or the average quality within 4bp window falling below quality scores 18 were trimmed. The
145 clean reads were aligned to reference genome *Apis mellifera* Amel_4.5
146 (https://www.ncbi.nlm.nih.gov/genome/48?genome_assembly_id=22683) by Bowtie 2 version 2.2.9
147 (Langmead and Salzberg, 2012). Another round of QC was performed on bam files. Library
148 complexity was checked by NRF (non-redundancy fraction), defined as the number of unique start
149 positions of uniquely mappable reads divided by number of uniquely mappable reads. All the samples
150 passed the threshold 0.8 recommended by ENCODE. IGVtools and bamCompare from deepTools
151 (Ramírez et al., 2014) were employed to compare two BAM files based on the number of mapped
152 reads. First the genome is partitioned into bins of equal size and then the number of reads in each bin is
153 counted. The log2 value for the ratio of number of reads per bin was reported for IGV visualization.
154 MACS2 was used for peaks calling with 0.01 FDR cutoff. Narrowpeak files as MACS2 output were
155 annotated by HOMER (Heinz et al., 2010). It first determines the distance to the nearest TSS and
156 assigns the peak to that gene. Then it determines the genomic annotation of the region covered by the
157 center of the peak, including TSS, TTS, Exon, Intronic, or Intergenic.

158 To test for non-random occurrence of peaks within genome features, we used 1000 random peak
159 datasets from the 7-day old worker data set. To create the random peak datasets, we used the shuffle
160 program of the BEDTools package (Aronesty, 2011) on the 782 peaks from the 7-day data set that were
161 located on full chromosome assemblies to generate 1000 bed files with peak locations that were

162 shuffled within chromosomes, such that shuffled peak locations were non-overlapping and did not
163 occur in assembly gaps. The `annotatePeaks.pl` program from the Homer package (Heinz et al., 2010)
164 was then used to annotate the 1000 shuffled peak data sets and the 7-day peak data set with respect to
165 genome features in the NCBI *Apis mellifera* RefSeq annotation. We used chi-squared tests to determine
166 whether the observed numbers of peaks overlapping promoter plus Transcription Start Site (TSS)
167 regions (-1 kb to +100 bp from TSS), Transcription Termination Sites (TTS), exons, introns and
168 intergenic regions were greater or less than expected by chance.

169

170 *2.9 Gene ontology*

171 We performed a gene ontology (GO) term analysis to determine if our list of Vg-DNA binding sites
172 was enriched for any biological processes, molecular functions, cellular components, or KEGG
173 pathways. We used the list of sites from 7-day old bees, but omitted sites found in *intergenic* regions.
174 Honey bee genes were converted to *D. melanogaster* orthologues (N = 360 genes), as this latter
175 genome is more robustly annotated. We used DAVID 6.8 (Huang et al., 2009) with default settings and
176 the resulting terms are those deemed significant ($P < 0.05$) after Benjamini-Hochberg corrections.

177

178 *2.10 Vg-DNA binding motif search*

179 For *de novo* motif identification, we created a non-redundant dataset of 790 peaks by combining peaks
180 identified in the newly emerged and 7-day old samples and merging peaks with overlapping regions
181 between the two datasets. We used GimmeMotifs (Heeringen et al., 2011) which ran and combined
182 results for ten motif prediction packages – Mdmodule, Weeder, GADEM, trawler, Improbizer,
183 BioProspector, Posmo, ChIPMunk, JASPAR, AMD, HMS and Homer. GimmeMotifs clusters the
184 results, performs enrichment and computes receiver operator characteristic (ROC) and mean
185 normalized conditional probability (MNCP). Half of the peaks (395) were used to train each algorithm

186 and the other half was used for testing. Since we did not have *a priori* knowledge of the motif length,
187 we ran GimmeMotifs four times with different size range options (small 5-8 bp, medium 5-12 bp, large
188 6-15 bp, xl 6-20 bp). Since the peaks were located throughout the genome, we used sequences
189 randomly chosen from the genome with GC content to the peak sequences as the background for the
190 enrichment tests.

191 2.11 *Vg response to immune challenge, enzymatic cleavage, and 3D structural model*

192 See S2.

193

194 3. Results

195 3.1. *Vg translocation to the nucleus*

196 3.1.1. *Immunohistology:*

197 We observed fat body cells using confocal microscopy (Fig 1A-E). Honey bee fat body contains two
198 cell types: Trophocytes are characterized by irregularly-shaped nuclei and are responsible for Vg
199 production and storage, while oenocytes have spherical nuclei and do not produce or contain Vg (Pan
200 et al., 1969; Roma et al., 2010). We observed two Vg localization patterns in trophocytes: i) Vg signal
201 co-localized with DAPI in the nucleus, and also found spread throughout the cytosol (Fig 1A-B), and
202 ii) Vg signal absent in the nucleus and instead restricted to granule-like formations in the cytosol (Fig
203 1C, see also (Havukainen et al., 2011) for observations of this pattern). Controls for autofluorescence
204 and unspecific secondary antibody staining were included (Fig 1D-E), which indicated that the
205 immunosignals present in Fig 1A-D are specific for Vg antibody incubation.

206

207 3.1.2. *Cell fractionation*

208 To verify the nuclear location of the Vg N-sheet, we separated fat body cells into cytosolic and nuclear
209 compartments by cell fractionation followed by western blot. Full-length Vg (180 kDa) and a ~75 kDa
210 band were found in the cytosolic component, while the nuclear component only contained fragments
211 below 75 kDa, including the 40 kDa N-sheet domain (Fig 2). We have shown previously that the 40
212 kDa Vg subunit is a specific cleavage product of fat body cells and not simply a biproduct of unspecific
213 degradation (Havukainen et al., 2012, 2011). We also observed 70, 37 and 25 kDa fragments in the
214 nuclear fraction, but these are likely degradation products caused by the method, as the bands are faint
215 or non-existent in untreated Western blot samples (see S1).

216

217 *3.1.3. Labeled whole Vg in cell culture*

218 To rule out that the nuclear signal was an artefact caused by Vg primary antibody, we incubated cell
219 cultures (Lepidopteran ovarian HighFive cells) with antibody-free pure fluorescently-labelled Vg.
220 During incubation, the fluorescent Vg was imported into cells and was visible in the cell nuclei co-
221 localizing with DAPI, and also visible in the cytosol in granule-like formations (Fig 3).

222

223 *3.2 Vg-DNA binding*

224 *3.2.1. In silico binding prediction*

225 Using the whole Vg amino acid sequence, two separate programs with different search algorithms, DP-
226 Bind (Hwang et al., 2007) and DRNApred (Yan and Kurgan, 2017), both identified the same amino
227 acid residue stretch as a putative DNA binding domain: SRSSTSR in position 250-256 of the N-sheet
228 domain of Vg. Another sequence-based program, DNABIND (Liu and Hu, 2013), also identified N-
229 terminal Vg as a DNA-binding protein. This program predicts a protein's DNA binding probability and
230 sets a threshold probably of 0.5896, above which a protein is statistically likely to be able to bind DNA.
231 Vg scored a 0.6267 probability, indicating it can bind DNA. Additionally, the structure-based

232 prediction software DISPLAR (Tjong and Zhou, 2007) identified the SRSSTSR stretch as capable of
233 binding DNA using a published honey bee Vg N-sheet model (Havukainen et al., 2011) as input. There
234 were another 12 and 3 additional stretches identified by DP-BIND and DRNApred, respectively, which
235 did not overlap between the programs, whereas DISPLAR identified two additional stretches that did
236 not overlap with predictions made by the two sequence-based programs. Taken together, results from
237 multiple prediction software platforms support the hypothesis that Vg can bind to DNA, and this
238 capability is likely restricted to the N-sheet.

239

240 3.2.2 *ChIP-seq*

241 ChIP DNA had significant enrichment (FDR < 0.01) at 90 and 782 putative Vg-DNA binding sites on
242 fully assembled chromosomes in newly emerged and 7-day old workers, respectively. Of the 90
243 binding sites in newly emerged bees, 83 (92%) were also present in 7-day old bees, illustrating an
244 expansion of Vg-DNA binding sites as workers age. Using the 7-day old worker binding sites, we
245 analyzed their genomic distribution compared to a null distribution of random peaks and found a
246 greater number than expected by chance within promotor-TSS, TTS, and intergenic regions, and fewer
247 than expected by chance in exons and introns (Fig 4).

248

249 3.2.3. *Gene Ontology*

250 Next, we again used the 7-day old worker binding sites to perform a Gene Ontology (GO)-term
251 analysis. We omitted binding sites located in intergenic regions and restricted our list to sites located in
252 or near genes (promotor regions, introns, exons, tts, N=574 binding sites across 484 genes). We
253 converted these *Apis mellifera* genes into *Drosophila melanogaster* orthologs (N=274 genes) using the
254 Hymenoptera Genome Database (Elsik et al., 2016) and used DAVID Bioinformatics Resources
255 (Huang et al., 2009) to look for enrichment of biological processes, molecular functions, cellular

256 components, and KEGG pathways. We found significant enrichment (Benjamini-Hochberg-corrected P
257 value < 0.05) for 142 terms and pathways (see Table S1). There was much overlap in these terms, but
258 most genes had functions pertaining to *developmental processes* (GO:0032502, N=134 genes, adj. P =
259 6.58 E-8), *neurogenesis* (GO:0022008, N=70 genes, adj. P = 4.63 E-8), *signaling* (GO:0023052, N=75
260 genes, adj. P = 4.74 E-5), or similar functions. Many genes bound by Vg code for membrane-bound
261 receptors that are known to play roles in complex phenotypes, like behavior, including receptors for
262 corazonin, glutamate, acetylcholine, serotonin, and octopamine (see Table S1 for complete list of Vg
263 binding sites). Furthermore, Vg was bound to more than a dozen immunological genes, including
264 *Defensin-1*, a key antimicrobial peptide, and *sickie*, an integral component of the Immune Deficiency
265 pathway defense against gram-negative bacteria. These results demonstrate that Vg binds to DNA at
266 hundreds of loci in the honey bee genome, that many are behaviorally-, developmentally-, and
267 immunologically-relevant, and that many of these Vg-DNA interactions persist as adult workers
268 transition between tasks.

269

270 3.2.4 Binding motif identification

271 We analyzed the binding site data to look for DNA sequences to which Vg may be binding. We ran
272 four analyses using GimmeMotif (Heeringen et al., 2011), and we selected the top motif predictions,
273 based on a combination of percent enrichment, P-value, ROC-AUC and MNCP (Table 1) (Fig 5). The
274 top motif prediction for the small motif run was a sub-motif of the large motif run, so it was discarded.
275 These results suggest that there are specific sequence motifs to which Vg binds.

276

277 Table 1. Top de novo motif predictions.

Motif	Enrichment	P-value	ROC-AUC *	MNCP*	Best Known Match	P-value for	No. Peaks with	Analysis
-------	------------	---------	-----------	-------	------------------	-------------	----------------	----------

							Match	motif	
TCAAGAGATGGCGC	35.75	6.36E-122	0.737	5.44	C2H2_ZF_M2196_1.01	5.27E-04	300	large	
nAkyrCCATCTnTyGrwwAn	34.5	2.12E-116	0.788	5.58	bHLH_Average_34	2.70E-02	310	medium	
TyAGCGCCATCT	33.1	2.81E-116	0.725	5.239	C2H2_ZF_M2196_1.01	8.10E-07	314	xl	

278 *ROC-AUC = area under ROC curve, MNCP = mean normalized conditional probability

279

280 3.3 *Vg cleavage dynamics*

281 3.3.1. *Vg protein cleavage and nuclear translocation in response to immune challenge:*

282 We found that Vg incubated *in vitro* with *E. coli* had increased protein fragmentation, but that worker
283 bees that ingested *E. coli* possessed fewer fat body nuclei with Vg signal within than workers fed a
284 control diet (see S2).

285

286 3.3.2. *Vg structure and enzymatic cleavage:*

287 We found that the linker region connecting the N-sheet with the rest of the Vg molecule protrudes from
288 the structure, providing easy access to proteolytic enzymes. Moreover, enzymatic cleavage is likely
289 carried out, at least partially, via dephosphorylation and caspase activity (see S2).

290

291 4. Discussion

292 Vg dates back at least 700 million years to the time when animals first appeared (Hayward et al.,
293 2010) (Fig 6), and the ubiquity of its roles in reproduction and immunity across diverse taxa (Du et al.,
294 2017; Li et al., 2008; Salmela et al., 2015) suggest that these functions developed early in its
295 evolutionary history. Several of its structural domains are highly conserved, and yet the molecular
296 mechanism by which Vg regulates so many complex traits like behavior and longevity has remained
297 something of a mystery. Here, we reveal a major and hitherto unknown ability of Vg that may provide

298 such a molecular explanation: nuclear translocation and DNA binding. Vg may be directly involved in
299 modulating gene expression, and given its prevalence in the animal kingdom and its conserved
300 molecular structure, it is possible that it performs a similar function across a wide array of oviparous
301 animals.

302
303 In our study, we found strong evidence of Vg translocating to the nucleus using three methods:
304 immunohistology, Western blot of proteins in the fractionated nuclear compartment, and antibody-free
305 localization of Vg in cell culture. The two first approaches confirmed the Vg N-sheet domain to be
306 present in both nucleus and cytosol, with the latter result reaffirming previous findings (Havukainen et
307 al., 2011). Moreover, the second approach specifies that the cell nucleus excludes the full length 180
308 kDa Vg molecule and the previously reported specific Vg fragmentation product of 150 kDa size (i.e.,
309 the Vg molecule without the N-sheet domain) (Havukainen et al., 2011). The cell culture approach
310 makes it less likely that antibody artefacts explain the outcomes of the first experiments.

311 We found theoretical support for Vg's DNA binding ability using several prediction software
312 platforms, and this prompted us to test this ability empirically. Our ChIP-seq analysis confirmed that
313 honey bee Vg binds to many loci in fat body DNA of newly emerged and 7-day old workers. Despite
314 there being far fewer Vg-DNA binding sites in newly emerged than 7-day old workers (150 vs 927 loci,
315 respectively), there is robust overlap in binding sites between these two age groups as over 90% of sites
316 observed in newly emerged workers are still present in 7-day older workers. This suggests that Vg not
317 only maintains long-term associations with specific loci, but also that the repertoire of Vg-DNA
318 binding sites expands as workers age and behaviorally transition from cell cleaning to nursing.

319 GO term analysis of Vg-DNA binding sites hint at the types of biological functions that Vg may
320 be targeting for regulation. We found significant enrichment for the GO terms *developmental processes*
321 (GO:0033502), *neurogenesis* (GO:0022008), and *signaling* (GO:0023052), among many others, and

322 many of the genes included within these terms code for membrane proteins. Indeed, many genes code
323 for G protein-coupled receptors and ion channels (Table S1), suggesting that Vg regulates components
324 of signal transduction pathways. Interestingly, newly emerged and 7-day old workers perform different
325 tasks, and many of these receptors are known to affect how individuals behave and respond to stimuli.
326 These include receptors for glutamate (Kucharski et al., 2007), acetylcholine (Eiri and Nieh, 2012),
327 corazonin (Gospocic et al., 2017), and octopamine (Grohmann et al., 2003). One possible explanation
328 is that as workers age and transition between tasks they respond to different signals from nestmates and
329 the environment, and thus must be equipped with relevant molecular machinery to receive and respond
330 to those signals.

331 A potential shortcoming here is that these Vg-DNA binding loci are from fat body cells rather
332 than neurons, so the effect on honey bee behavior might appear limited. However, Vg is neither found
333 nor expressed in honey bee neurons (Münch et al., 2015), limiting its likelihood of binding to DNA
334 therein. Fat body, on the other hand, not only produces and stores Vg, but also plays a central role in
335 regulating metabolism and homeostasis. In this capacity, it produces many products that affect a wide
336 range of insect behaviors, including courtship (Lazareva et al., 2007), host-seeking (Klowden et al.,
337 1987), and onset of foraging (Antonio et al., 2008). Moreover, the fat body is a key player in innate
338 immunity (Fehlbaum et al., 1994; Lycett et al., 2006; Morishima et al., 1997), and our data show Vg to
339 be bound to several important immune-related genes in this tissue. These include *defensin-1*, an
340 important antimicrobial peptide (Ganz, 2003), *sickie*, a regulator of immune transcription factors (Foley
341 and O'Farrell, 2004), and several genes involved in autophagy and phagocytosis (Levine and Deretic,
342 2007; Strand, 2008)(Table S1). Taken together, the fat body's central role in honey bee biology means
343 that any protein-DNA binding herein could have wide-ranging effects on numerous physiological
344 pathways. This work also revealed several putative *de novo* DNA binding motifs for Vg. The aim of
345 this ChIP-seq work here was to determine whether Vg binds to DNA, and if so, at which loci. Our next

346 step is to further our understanding of Vg's actions inside the nucleus and to determine how it regulates
347 gene expression across different caste types and populations in honey bees. This is a multi-faceted
348 approach that will involve performing ChIP-seq on workers, drones, and queens from multiple colonies
349 to determine how Vg differentially binds to DNA, and performing gene expression analyses such as
350 RNA-seq to elucidate how Vg-DNA binding up- or down-regulates gene expression at various loci.
351 Furthermore, we can distinguish whether Vg is a transcription factor or co-regulator by determining
352 what other proteins it interacts with in the nucleus via co-immunoprecipitation and mass spectrometry
353 (Li et al., 2016). This will greatly enhance our knowledge of Vg's regulatory properties and can
354 potentially unveil co-evolutionary relationships between Vg and other proteins. Nevertheless, the
355 findings presented in this study here represent a major new discovery of Vg function.

356 Our discovery that the Vg N-sheet subunit binds to DNA in fat body cell nuclei raises several
357 questions that warrant further research. First, does Vg translocate into the nucleus in other tissues in
358 addition to the fat body? Vg has been verified in eggs and ovaries (Seehuus et al., 2007), in
359 hypopharyngeal glands (Seehuus et al., 2007), in immune cells (Hystad et al., 2017), and in glial cells
360 of the honey bee brain (Münch et al., 2015). In this latter observation, it is specifically the Vg N-sheet
361 that is localized in glial cells, and such subcellular localization should prompt a highly relevant
362 research subject since honey bee *vg* knock-downs show an altered brain gene expression pattern
363 (Wheeler et al., 2013) and major behavioral changes (Nelson et al., 2007). Second, does Vg naturally
364 translocate to the nucleus in other animals? The N-terminal Vg cleavage pattern is similar in most
365 insects studied (Tufail and Takeda, 2008), but the possibility of N-sheet translocation remains
366 speculative before it is experimentally tested in another species. Finally, what role do other Vg
367 fragments play in nuclear translocation? The N-sheet-specific antibodies, as well as Vg purified from
368 fat body, show weak protein bands smaller in size to full-length Vg, most notably, bands of ~75 and
369 ~125 kDa in size. It is unclear if these are functional Vg fragments or simply the result of unspecific

370 fragmentation. In general, we have observed that Vg fragment number grows in harsh sample treatment
371 conditions. We suspect that at least a 25 kDa fragment detected by the Vg antibody used here in our
372 tissue fractioning assay is a degradation product caused by the assay protocol. However, it is not ruled
373 out that other Vg fragments in addition to N-sheet play a role in nuclear localization of Vg.

374 Vg was first discovered as an egg-yolk protein, but the protein is so ancient that we cannot be
375 certain of its original function, and it is possible that it assumed a gene regulatory role via DNA-
376 binding early in its history. While we only touch on the mechanistic link between Vg and its
377 multifunctionality, our results will hopefully spark diverse future studies on the role of Vg as a putative
378 transcription factor in honey bees and other animal species.

379

380

381 **5. Acknowledgements**

382 MSc Taina Stark assisted with the *in vivo* assay. The inhibitors were kind courtesy of Professor
383 Matthew Bogyo at Stanford University, USA. We thank Professor Bogyo and his lab members, as well
384 as Prof. Guy Salvesen (Sanford-Burnham, USA) and Professor Christopher Overall (University of
385 British Columbia, Canada) for advice and innovative discussions. We thank Claus Kreibich
386 (Norwegian University of Life Sciences, Norway), Nicholas Boss (Arizona State University, USA),
387 Osman Kaftanoglu, (Arizona State University, USA), Cahit Ozturk (Arizona State University, USA),
388 Eero Hänninen, Finnish Beekeepers' Association and Stadin Tarhaajat association for assisting with the
389 live honey bee samples. Thanks to Professor Michelle Krogsgaard (New York University, USA) for
390 help and advice with insect cell culturing, and Dr. Dimitri Stucki for assistance with the statistical test.
391 We also thank Dr. Hua Bai (Iowa State University, USA) and Marc Tatar (Brown University, USA) for
392 insight and training on chromatin immuno-precipitation, as well as Dr. Jason Steele, Dr. Shanshan

393 Yang, and the DNASU Next Generation Sequencing Core (Arizona State University, USA) for
394 sequencing and initial bioinformatics.

395
396 **6. Declarations**

397 **6.1 Funding**

398 HS was supported by Academy of Finland (#265971). GH was supported by the Natural Sciences and
399 Engineering Research Council of Canada (#376088068) and the School of Life Sciences Research
400 Training Initiative at Arizona State University (#LM5 1079_GH). GA was supported by the Research
401 Council of Norway (#262137).

402

403 **6.2 Conflicts of interest**

404 The authors declare no conflicts of interest.

405

406 **6.3 Availability of data**

407 All relevant experimental data are included in the manuscript and supplementary materials. 3D
408 structural model of Vg is deposited in the Worldwide Protein Data Bank (D_1000249604).

409

410 **6.4 Ethics approval**

411 Not applicable

412

413 **6.5 Consent to participate**

414 Not applicable

415

416 **6.6 Consent for publication**

417 Not applicable

418

419 6.7 Author's contributions

420 GH, HS, and GA conceived this research and designed experiments; HS, GH, DM, CE, EHG and MV
421 performed experiments and analysis; GH and HS wrote the paper; GH made revisions. GA oversaw the
422 project.

423

424

425

426

427

428

429

430

431

432

433

434

435

436

437

438

439

440

441

442

443

444

445 **References**

446 Agnese, M., Verderame, M., De Meo, E., Prisco, M., Rosati, L., Limatola, E., del Gaudio, R., Aceto,
447 S., Andreuccetti, P., 2013. A network system for vitellogenin synthesis in the mussel *Mytilus*
448 *galloprovincialis* (L.). *J. Cell. Physiol.* 228, 547–555.

449 Akasaka, M., Kato, K.H., Kitajima, K., Sawada, H., 2013. Identification of Novel Isoforms of
450 Vitellogenin Expressed in Ascidian Eggs. *J. Exp. Zoolog. B Mol. Dev. Evol.* 320, 118–128.
451 <https://doi.org/10.1002/jez.b.22488>

452 Amdam, G.V., Norberg, K., Page Jr., R.E., Erber, J., Scheiner, R., 2006. Downregulation of
453 vitellogenin gene activity increases the gustatory responsiveness of honey bee workers (*Apis*
454 *mellifera*). *Behav. Brain Res.* 169, 201–205. <https://doi.org/10.1016/j.bbr.2006.01.006>

455 Amdam, G.V., Omholt, S.W., 2002. The Regulatory Anatomy of Honeybee Lifespan. *J. Theor. Biol.*
456 216, 209–228. <https://doi.org/10.1006/jtbi.2002.2545>

457 Andrews, S., 2010. FastQC A Quality Control tool for High Throughput Sequence Data [WWW
458 Document]. URL <https://www.bioinformatics.babraham.ac.uk/projects/fastqc/> (accessed
459 10.12.18).

460 Antonio, D.S.M., Guidugli-Lazzarini, K.R., Nascimento, A.M. do, Simões, Z.L.P., Hartfelder, K.,
461 2008. RNAi-mediated silencing of vitellogenin gene function turns honeybee (*Apis mellifera*)
462 workers into extremely precocious foragers. *Naturwissenschaften* 95, 953–961.
463 <https://doi.org/10.1007/s00114-008-0413-9>

464 Aronesty, E., 2011. ea-utils: Command-line tools for processing biological sequencing data.
465 Babin, P.J., 2008. Conservation of a vitellogenin gene cluster in oviparous vertebrates and
466 identification of its traces in the platypus genome. *Gene* 413, 76–82.
467 <https://doi.org/10.1016/j.gene.2008.02.001>

468 Bai, H., Kang, P., Hernandez, A.M., Tatar, M., 2013. Activin Signaling Targeted by Insulin/dFOXO
469 Regulates Aging and Muscle Proteostasis in *Drosophila*. *PLOS Genet.* 9, e1003941.
470 <https://doi.org/10.1371/journal.pgen.1003941>

471 Baker, M.E., 1988. Is vitellogenin an ancestor of apolipoprotein B-100 of human low-density
472 lipoprotein and human lipoprotein lipase? *Biochem. J.* 255, 1057–1060.

473 Biscotti, M.A., Barucca, M., Carducci, F., Canapa, A., 2018. New Perspectives on the Evolutionary
474 History of Vitellogenin Gene Family in Vertebrates. *Genome Biol. Evol.* 10, 2709–2715.
475 <https://doi.org/10.1093/gbe/evy206>

476 Bolger, A.M., Lohse, M., Usadel, B., 2014. Trimmomatic: a flexible trimmer for Illumina sequence
477 data. *Bioinformatics* 30, 2114–2120. <https://doi.org/10.1093/bioinformatics/btu170>

478 Brawand, D., Wahli, W., Kaessmann, H., 2008. Loss of Egg Yolk Genes in Mammals and the Origin of
479 Lactation and Placentation. *PLOS Biol.* 6, e63. <https://doi.org/10.1371/journal.pbio.0060063>

480 Chen, C., Li, H.-W., Ku, W.-L., Lin, C.-J., Chang, C.-F., Wu, G.-C., 2018. Two distinct vitellogenin
481 genes are similar in function and expression in the bigfin reef squid *Sepioteuthis lessoniana*.
482 *Biol. Reprod.* 99, 1034–1044. <https://doi.org/10.1093/biolre/foy131>

483 Chen, J.-S., Sappington, T.W., Raikhel, A.S., 1997. Extensive sequence conservation among insect,
484 nematode, and vertebrate vitellogenins reveals ancient common ancestry. *J. Mol. Evol.* 44, 440–
485 451.

486 Chesmore, K.N., Bartlett, J., Cheng, C., Williams, S.M., 2016. Complex Patterns of Association
487 between Pleiotropy and Transcription Factor Evolution. *Genome Biol. Evol.* 8, 3159–3170.
488 <https://doi.org/10.1093/gbe/evw228>

489 Du, X., Wang, X., Wang, S., Zhou, Y., Zhang, Y., Zhang, S., 2017. Functional characterization of
490 Vitellogenin_N domain, domain of unknown function 1943, and von Willebrand factor type D
491 domain in vitellogenin of the non-bilaterian coral *Euphyllia ancora*: Implications for emergence
492 of immune activity of vitellogenin in basal metazoan. *Dev. Comp. Immunol.* 67, 485–494.
493 <https://doi.org/10.1016/j.dci.2016.10.006>

494 Eiri, D.M., Nieh, J.C., 2012. A nicotinic acetylcholine receptor agonist affects honey bee sucrose
495 responsiveness and decreases waggle dancing. *J. Exp. Biol.* 215, 2022–2029.
496 <https://doi.org/10.1242/jeb.068718>

497 Elsik, C.G., Tayal, A., Diesh, C.M., Unni, D.R., Emery, M.L., Nguyen, H.N., Hagen, D.E., 2016.
498 Hymenoptera Genome Database: integrating genome annotations in HymenopteraMine.
499 *Nucleic Acids Res.* 44, D793–D800. <https://doi.org/10.1093/nar/gkv1208>

500 Fehlbaum, P., Bulet, P., Michaut, L., Lagueux, M., Broekaert, W.F., Hetru, C., Hoffmann, J.A., 1994.
501 Insect immunity. Septic injury of *Drosophila* induces the synthesis of a potent antifungal
502 peptide with sequence homology to plant antifungal peptides. *J. Biol. Chem.* 269, 33159–
503 33163.

504 Foley, E., O'Farrell, P.H., 2004. Functional Dissection of an Innate Immune Response by a Genome-
505 Wide RNAi Screen. *PLOS Biol.* 2, e203. <https://doi.org/10.1371/journal.pbio.0020203>

506 Ganz, T., 2003. Defensins: antimicrobial peptides of innate immunity. *Nat. Rev. Immunol.* 3, 710–720.
507 <https://doi.org/10.1038/nri1180>

508 Garcia, J., Munro, E.S., Monte, M.M., Fourrier, M.C.S., Whitelaw, J., Smail, D.A., Ellis, A.E., 2010.
509 Atlantic salmon (*Salmo salar* L.) serum vitellogenin neutralises infectivity of infectious
510 pancreatic necrosis virus (IPNV). *Fish Shellfish Immunol.* 29, 293–297.
511 <https://doi.org/10.1016/j.fsi.2010.04.010>

512 García-Alonso, J., Hoeger, U., Rebscher, N., 2006. Regulation of vitellogenesis in *Nereis virens*
513 (Annelida: Polychaeta): Effect of estradiol-17 β on eleocytes. *Comp. Biochem. Physiol. A. Mol.*
514 *Integr. Physiol.* 143, 55–61. <https://doi.org/10.1016/j.cbpa.2005.10.022>

515 Gospocic, J., Shields, E.J., Glastad, K.M., Lin, Y., Penick, C.A., Yan, H., Mikheyev, A.S., Linksvayer,
516 T.A., Garcia, B.A., Berger, S.L., Liebig, J., Reinberg, D., Bonasio, R., 2017. The Neuropeptide
517 Corazonin Controls Social Behavior and Caste Identity in Ants. *Cell* 170, 748–759.e12.
518 <https://doi.org/10.1016/j.cell.2017.07.014>

519 Grohmann, L., Blenau, W., Erber, J., Ebert, P.R., Strünker, T., Baumann, A., 2003. Molecular and
520 functional characterization of an octopamine receptor from honeybee (*Apis mellifera*) brain. *J.*
521 *Neurochem.* 86, 725–735. <https://doi.org/10.1046/j.1471-4159.2003.01876.x>

522 Havukainen, H., Halskau, Ø., Skjaerven, L., Smedal, B., Amdam, G.V., 2011. Deconstructing
523 honeybee vitellogenin: novel 40 kDa fragment assigned to its N terminus. *J. Exp. Biol.* 214,
524 582–592. <https://doi.org/10.1242/jeb.048314>

525 Havukainen, H., Münch, D., Baumann, A., Zhong, S., Halskau, Ø., Krogsgaard, M., Amdam, G.V.,
526 2013. Vitellogenin Recognizes Cell Damage through Membrane Binding and Shields Living
527 Cells from Reactive Oxygen Species. *J. Biol. Chem.* 288, 28369–28381.
528 <https://doi.org/10.1074/jbc.M113.465021>

529 Havukainen, H., Underhaug, J., Wolschin, F., Amdam, G., Halskau, Ø., 2012. A vitellogenin
530 polyserine cleavage site: highly disordered conformation protected from proteolysis by
531 phosphorylation. *J. Exp. Biol.* 215, 1837–1846. <https://doi.org/10.1242/jeb.065623>

532 Hayward, A., Takahashi, T., Bendena, W.G., Tobe, S.S., Hui, J.H.L., 2010. Comparative genomic and
533 phylogenetic analysis of vitellogenin and other large lipid transfer proteins in metazoans. *FEBS*
534 *Lett.* 584, 1273–1278. <https://doi.org/10.1016/j.febslet.2010.02.056>

535 Heeringen, V., J. S., Veenstra, G.J.C., 2011. GimmeMotifs: a de novo motif prediction pipeline for
536 ChIP-sequencing experiments. *Bioinformatics* 27, 270–271.
537 <https://doi.org/10.1093/bioinformatics/btq636>

538 Heinz, S., Benner, C., Spann, N., Bertolino, E., Lin, Y.C., Laslo, P., Cheng, J.X., Murre, C., Singh, H.,
539 Glass, C.K., 2010. Simple Combinations of Lineage-Determining Transcription Factors Prime
540 cis-Regulatory Elements Required for Macrophage and B Cell Identities. *Mol. Cell* 38, 576–
541 589. <https://doi.org/10.1016/j.molcel.2010.05.004>

542 Huang, D.W., Sherman, B.T., Lempicki, R.A., 2009. Systematic and integrative analysis of large gene
543 lists using DAVID bioinformatics resources. *Nat. Protoc.* 4, 44–57.
544 <https://doi.org/10.1038/nprot.2008.211>

545 Hwang, S., Gou, Z., Kuznetsov, I.B., 2007. DP-Bind: a web server for sequence-based prediction of
546 DNA-binding residues in DNA-binding proteins. *Bioinformatics* 23, 634–636.
547 <https://doi.org/10.1093/bioinformatics/btl672>

548 Hystad, E.M., Salmela, H., Amdam, G.V., Münch, D., 2017. Hemocyte-mediated phagocytosis differs
549 between honey bee (*Apis mellifera*) worker castes. *PLOS ONE* 12, e0184108.
550 <https://doi.org/10.1371/journal.pone.0184108>

551 Jensen, P.V., Børgesen, L.W., 2000. Regional and functional differentiation in the fat body of
552 pharaoh's ant queens, *Monomorium pharaonis* (L.). *Arthropod Struct. Dev.* 29, 171–184.
553 [https://doi.org/10.1016/S1467-8039\(00\)00021-9](https://doi.org/10.1016/S1467-8039(00)00021-9)

554 Klowden, M.J., Davis, E.E., Bowen, M.F., 1987. Role of the fat body in the regulation of host-seeking
555 behaviour in the mosquito, *Aedes aegypti*. *J. Insect Physiol.* 33, 643–646.
556 [https://doi.org/10.1016/0022-1910\(87\)90133-8](https://doi.org/10.1016/0022-1910(87)90133-8)

557 Kucharski, R., Mitri, C., Grau, Y., Maleszka, R., 2007. Characterization of a metabotropic glutamate
558 receptor in the honeybee (<Emphasis Type="Italic">Apis mellifera</Emphasis>): implications
559 for memory formation. *Invert. Neurosci.* 7, 99–108. <https://doi.org/10.1007/s10158-007-0045-3>

560 Langmead, B., Salzberg, S.L., 2012. Fast gapped-read alignment with Bowtie 2. *Nat. Methods* 9, 357–
561 359. <https://doi.org/10.1038/nmeth.1923>

562 Lazareva, A.A., Roman, G., Mattox, W., Hardin, P.E., Dauwalder, B., 2007. A Role for the Adult Fat
563 Body in *Drosophila* Male Courtship Behavior. *PLOS Genet.* 3, e16.
564 <https://doi.org/10.1371/journal.pgen.0030016>

565 Levine, B., Deretic, V., 2007. Unveiling the roles of autophagy in innate and adaptive immunity. *Nat.*
566 *Rev. Immunol.* 7, 767–777. <https://doi.org/10.1038/nri2161>

567 Li, A., Sadasivam, M., Ding, J.L., 2003. Receptor-Ligand Interaction between Vitellogenin Receptor
568 (VtgR) and Vitellogenin (Vtg), Implications on Low Density Lipoprotein Receptor and
569 Apolipoprotein B/E THE FIRST THREE LIGAND-BINDING REPEATS OF VTGR
570 INTERACT WITH THE AMINO-TERMINAL REGION OF VTG. *J. Biol. Chem.* 278, 2799–
571 2806. <https://doi.org/10.1074/jbc.M205067200>

572 Li, Y., Collins, M., An, J., Geiser, R., Tegeler, T., Tsantilas, K., Garcia, K., Pirrotte, P., Bowser, R.,
573 2016. Immunoprecipitation and mass spectrometry defines an extensive RBM45 protein–
574 protein interaction network. *Brain Res., RNA Metabolism in Neurological Disease* 1647, 79–
575 93. <https://doi.org/10.1016/j.brainres.2016.02.047>

576 Li, Z., Zhang, S., Liu, Q., 2008. Vitellogenin Functions as a Multivalent Pattern Recognition Receptor
577 with an Opsonic Activity. *PLoS ONE* 3, e1940. <https://doi.org/10.1371/journal.pone.0001940>

578 Liu, R., Hu, J., 2013. DNABind: A hybrid algorithm for structure-based prediction of DNA-binding
579 residues by combining machine learning- and template-based approaches. *Proteins Struct.*
580 *Funct. Bioinforma.* 81, 1885–1899. <https://doi.org/10.1002/prot.24330>

581 Lycett, G.J., McLaughlin, L.A., Ranson, H., Hemingway, J., Kafatos, F.C., Loukeris, T.G., Paine,
582 M.J.I., 2006. *Anopheles gambiae* P450 reductase is highly expressed in oenocytes and in vivo
583 knockdown increases permethrin susceptibility. *Insect Mol. Biol.* 15, 321–327.
584 <https://doi.org/10.1111/j.1365-2583.2006.00647.x>

585 Morishima, I., Yamano, Y., Inoue, K., Matsuo, N., 1997. Eicosanoids mediate induction of immune
586 genes in the fat body of the silkworm, *Bombyx mori*. *FEBS Lett.* 419, 83–86.
587 [https://doi.org/10.1016/S0014-5793\(97\)01418-X](https://doi.org/10.1016/S0014-5793(97)01418-X)

588 Münch, D., Ihle, K.E., Salmela, H., Amdam, G.V., 2015. Vitellogenin in the honey bee brain: Atypical
589 localization of a reproductive protein that promotes longevity. *Exp. Gerontol., Aging in the*
590 *Wild: Insights from Free-Living and Non-Model organisms* 71, 103–108.
591 <https://doi.org/10.1016/j.exger.2015.08.001>

592 Nelson, C.M., Ihle, K.E., Fondrk, M.K., Page, R.E., Jr., Amdam, G.V., 2007. The Gene vitellogenin
593 Has Multiple Coordinating Effects on Social Organization. *PLoS Biol* 5, e62.
594 <https://doi.org/10.1371/journal.pbio.0050062>

595 Pan, M.L., Bell, W.J., Telfer, W.H., 1969. Vitellogenin Blood Protein Synthesis by Insect Fat Body.
596 *Science* 165, 393–394. <https://doi.org/10.1126/science.165.3891.393>

597 Prowse, T.A., Byrne, M., 2012. Evolution of yolk protein genes in the Echinodermata. *Evol. Dev.* 14,
598 139–151.

599 Ramírez, F., Dündar, F., Diehl, S., Grüning, B.A., Manke, T., 2014. deepTools: a flexible platform for
600 exploring deep-sequencing data. *Nucleic Acids Res.* 42, W187–W191.
601 <https://doi.org/10.1093/nar/gku365>

602 Riesgo, A., Farrar, N., Windsor, P.J., Giribet, G., Leys, S.P., 2014. The Analysis of Eight
603 Transcriptomes from All Poriferan Classes Reveals Surprising Genetic Complexity in Sponges.
604 *Mol. Biol. Evol.* 31, 1102–1120. <https://doi.org/10.1093/molbev/msu057>

605 Roma, G.C., Bueno, O.C., Camargo-Mathias, M.I., 2010. Morpho-physiological analysis of the insect
606 fat body: A review. *Micron* 41, 395–401. <https://doi.org/10.1016/j.micron.2009.12.007>

607 Salmela, H., Amdam, G.V., Freitak, D., 2015. Transfer of Immunity from Mother to Offspring Is
608 Mediated via Egg-Yolk Protein Vitellogenin. *PLoS Pathog* 11, e1005015.
609 <https://doi.org/10.1371/journal.ppat.1005015>

610 Salmela, H., Stark, T., Stucki, D., Fuchs, S., Freitak, D., Dey, A., Kent, C.F., Zayed, A., Dhaygude, K.,
611 Hokkanen, H., Sundström, L., 2016. Ancient Duplications Have Led to Functional Divergence
612 of Vitellogenin-Like Genes Potentially Involved in Inflammation and Oxidative Stress in
613 Honey Bees. *Genome Biol. Evol.* 8, 495–506. <https://doi.org/10.1093/gbe/evw014>

614 Sappington, T.W., 2002. The major yolk proteins of higher diptera are homologs of a class of minor
615 yolk proteins in lepidoptera. *J. Mol. Evol.* 55, 470–475.

616 Seehuus, S.-C., Norberg, K., Krekling, T., Fondrk, K., Amdam, G.V., 2007. Immunogold Localization
617 of Vitellogenin in the Ovaries, Hypopharyngeal Glands and Head Fat Bodies of Honeybee
618 Workers, *Apis Mellifera*. *J. Insect Sci.* 7, 1–14. <https://doi.org/10.1673/031.007.5201>

619 Strand, M.R., 2008. The insect cellular immune response. *Insect Sci.* 15, 1–14.
620 <https://doi.org/10.1111/j.1744-7917.2008.00183.x>

621 Tjong, H., Zhou, H.-X., 2007. DISPLAR: an accurate method for predicting DNA-binding sites on
622 protein surfaces. *Nucleic Acids Res.* 35, 1465–1477. <https://doi.org/10.1093/nar/gkm008>

623 Tufail, M., Takeda, M., 2008. Molecular characteristics of insect vitellogenins. *J. Insect Physiol.* 54,
624 1447–1458. <https://doi.org/10.1016/j.jinsphys.2008.08.007>

625 Wang, R., Brattain, M.G., 2007. The maximal size of protein to diffuse through the nuclear pore is
626 larger than 60 kDa. *FEBS Lett.* 581, 3164–3170. <https://doi.org/10.1016/j.febslet.2007.05.082>

627 Wheeler, M.M., Ament, S.A., Rodriguez-Zas, S.L., Robinson, G.E., 2013. Brain gene expression
628 changes elicited by peripheral vitellogenin knockdown in the honey bee. *Insect Mol. Biol.* 22,
629 562–573. <https://doi.org/10.1111/imb.12043>

630 Xu, J., Kudron, M.M., Victorsen, A., Gao, J., Ammour, H.N., Navarro, F.C.P., Gevirtzman, L.,
631 Waterston, R.H., White, K.P., Reinke, V., Gerstein, M., 2021. To mock or not: a comprehensive
632 comparison of mock IP and DNA input for ChIP-seq. *Nucleic Acids Res.* 49, e17–e17.
633 <https://doi.org/10.1093/nar/gkaa1155>

634 Yan, J., Kurgan, L., 2017. DRNApred, fast sequence-based method that accurately predicts and
635 discriminates DNA- and RNA-binding residues. *Nucleic Acids Res.* 45, e84.
636 <https://doi.org/10.1093/nar/gkx059>

637

Figures Captions:

Fig 1. Localization of Vg signals in the honey bee fat body using an antibody targeting the N-terminal 40 kDa domain. A-E Confocal images of fat body cells representing six samples. The last panel shows the superposition of DAPI (cyan) and Vg signal (red). A: Vg signal co-localizes with DAPI in cell nuclei. B: Zoom-in of a single cell showing Vg nuclear translocation. C: Cells that do not show Vg co-localization with DAPI, instead, Vg signal is found in granules in the cytosol. The scale bar = 10 μ m. D-E show representative images for controls where the primary antibody was applied (D) or omitted (E). Note that when omitting Vg antibody incubation, no immunosignal was detected (grayscale), while only the DAPI signal (cyan) was present. Scalebar = 50 μ m. Magnification 40x.

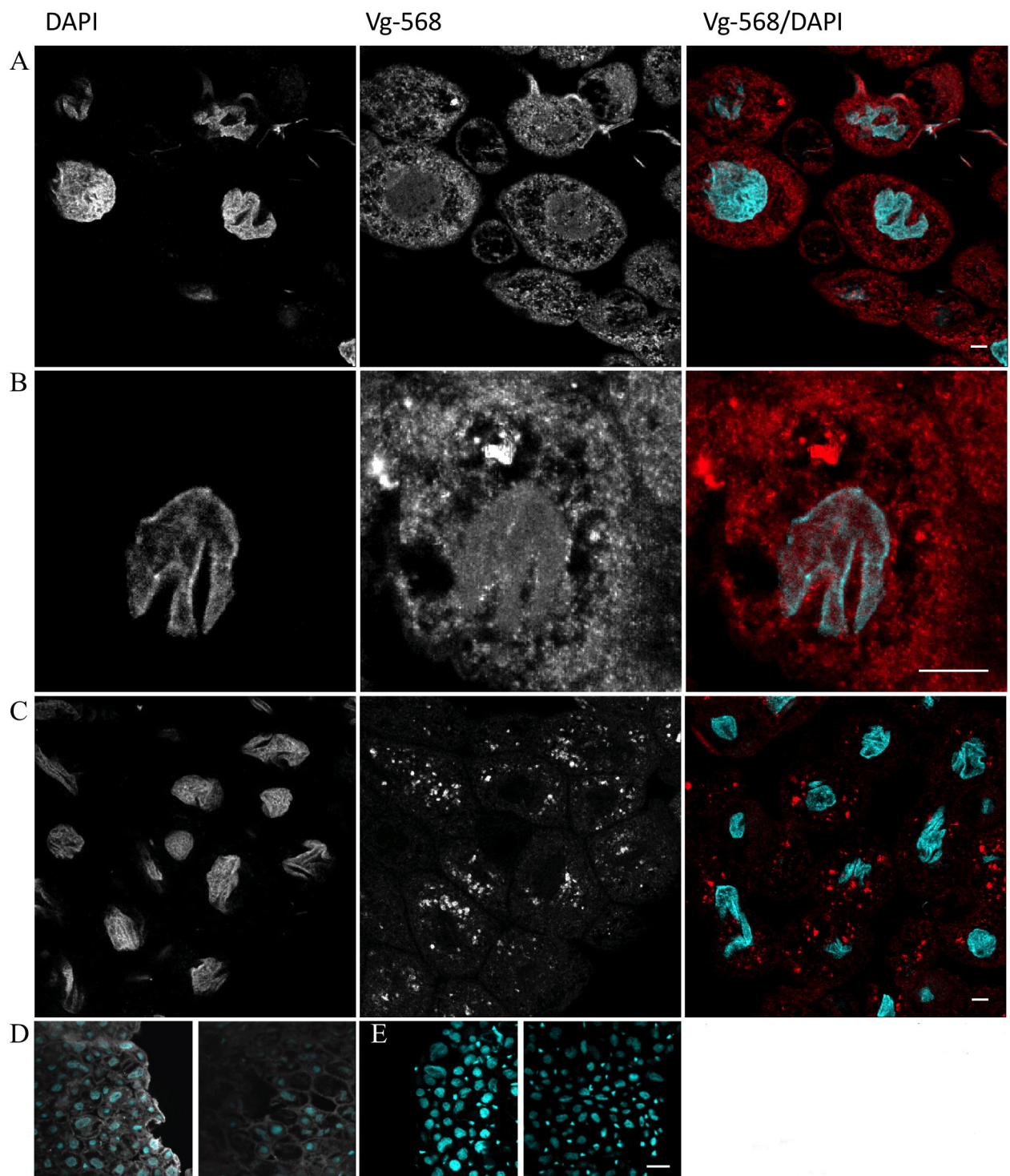
Fig 2. Western blot of cytosolic and nuclear fractions of honey bee fat body tissue. St. = size standard. The full-length (180 kDa) Vg is dominating the cytosolic fraction of the fat body proteins, whereas the 40-kDa N-terminal fragment mostly localizes in the nuclear fraction. Also, other fragments of approximately 70 and 25 kDa were visible in the nuclear fraction. Three individuals were pooled for each lane. N = 3.

Fig 3. Localization of Alexa-488-labelled purified Vg in cultured insect HighFive cells. Vg was observed both in cytosol mostly in bright granules and as haze in the nucleus in the confocal sections. The lowest row shows two Vg-negative controls imaged with the same settings. Scale bar = 5 μ m. Magnification 63x.

Fig 4. Genomic distribution of observed Vg-DNA binding sites compared with a null distribution. The null distribution was created by randomly shuffling 782 non-overlapping ChIP-seq peaks for 1000 iterations. We found more Vg-DNA binding sites than expected by chance in promotor regions ($\chi^2 = 175.18$, $P = 5.47\text{E-}40$), transcription termination sites ($\chi^2 = 91.68$, $P = 2.09\text{E-}24$), and intergenic regions ($\chi^2 = 46.14$, $P = 1.10\text{E-}11$), and fewer than expected by chance in exons ($\chi^2 = 3.75$, $P = 0.05$) and introns ($\chi^2 = 244.55$, $P = 4.01\text{E-}55$)

Fig 5. Logo representations for the top motif predictions. A) Top motif prediction from analysis with “large” motif setting (35.75% enrichment). B) Top motif prediction from analysis with “medium” motif setting (34.5% enrichment). C) Top motif prediction from analysis with “xl” motif setting (33.1% enrichment).

Fig 6. The deep phylogenetic history of Vitellogenin. Vg first evolved around 700 million years ago when Metazoans appeared (Hayward et al., 2010) and is present in all extant Metazoan phyla, from earliest animals like sponges and cnidarians to the more recently evolved chordates, like fish, birds, and monotreme mammals (Agnese et al., 2013; Akasaka et al., 2013; Babin, 2008; Biscotti et al., 2018; Chen et al., 2018, 1997; García-Alonso et al., 2006; Prowse and Byrne, 2012; Riesgo et al., 2014). Vg has been lost in several scientifically important lineages, including placental mammals and higher dipterans like *D. melanogaster* (depicted with dashed yellow lines) (Brawand et al., 2008; Sappington, 2002). Vg’s earliest known functions pertain to egg-yolk formation and immunity, but it remains to be seen when DNA binding evolved.



St.

Cytosolic

Nuclear

kDa



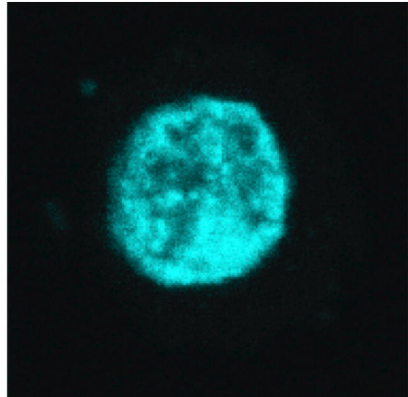
180



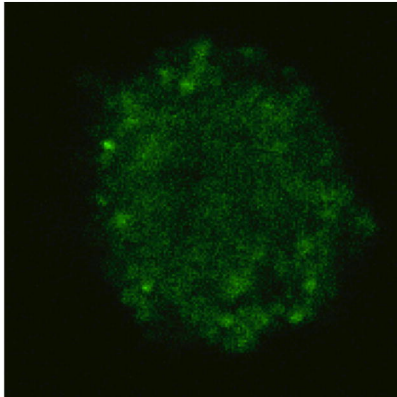
40



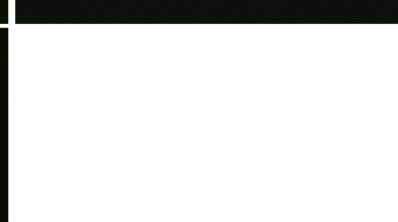
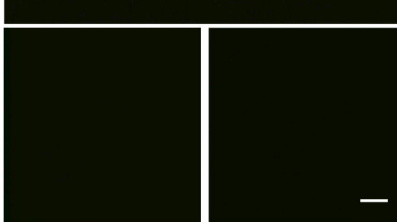
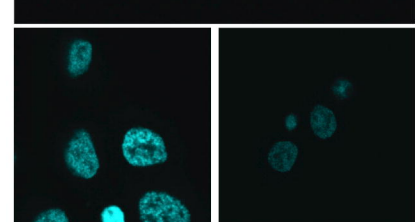
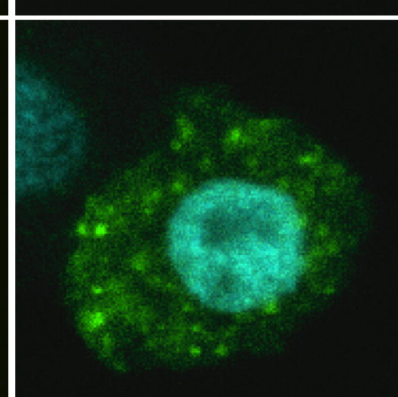
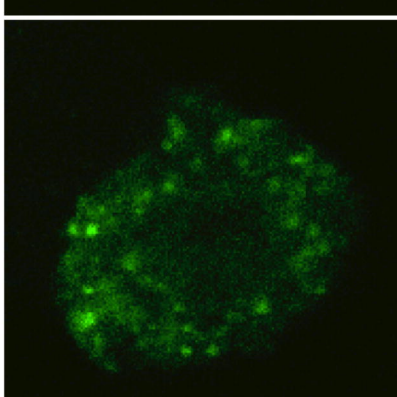
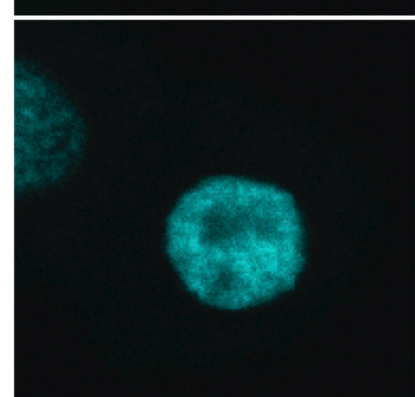
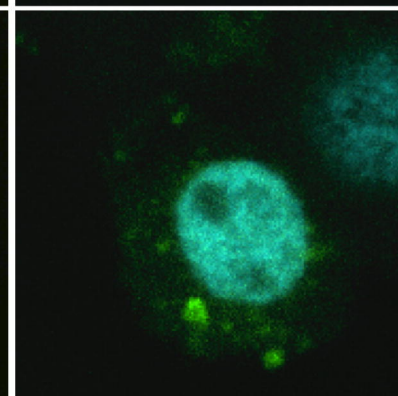
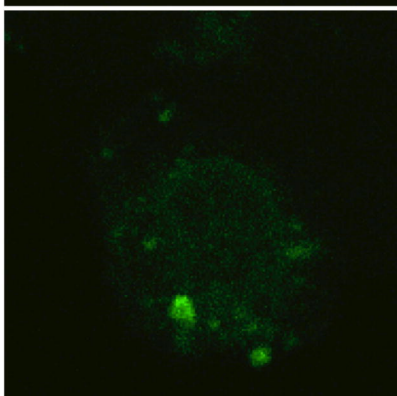
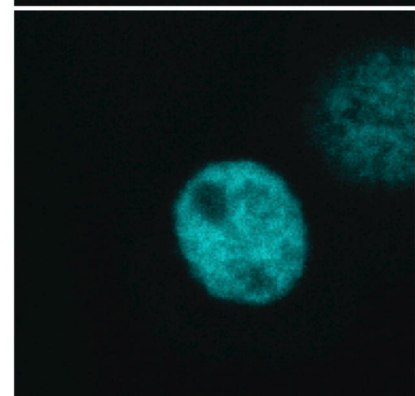
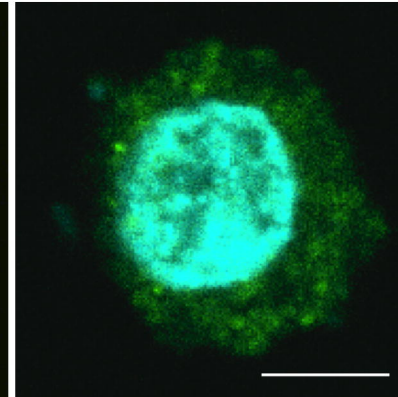
DAPI



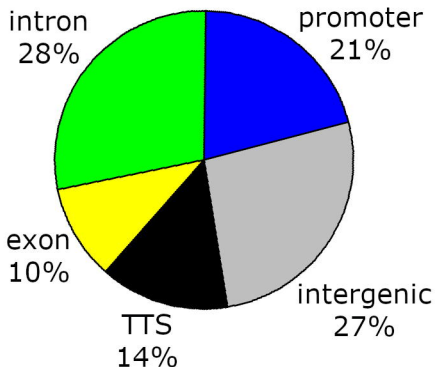
Vg-488



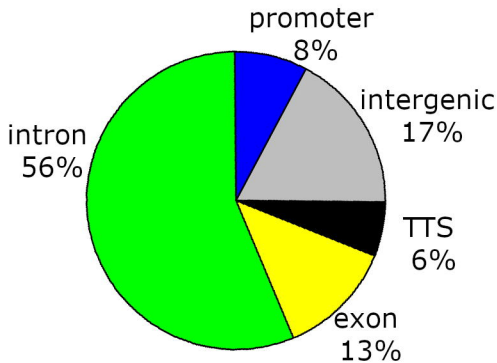
DAPI/Vg-488



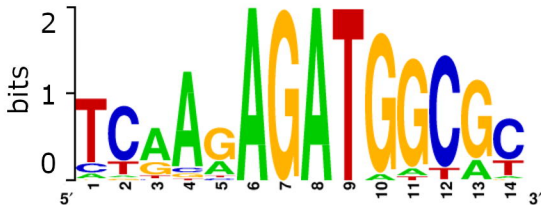
Observed Distribution



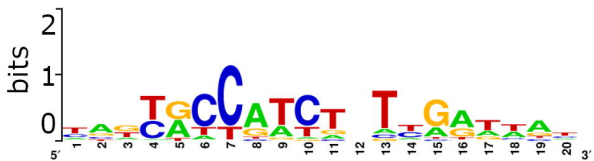
Expected (null) Distribution



A



B



C

